Article
Vol. 25, No. 6, p. 813–829, December 2021
https://doi.org/10.1007/s12303-021-0006-6
pISSN 1226-4806 eISSN 1598-7477
Geosciences Journal GJ

Some geomorphic indices in the North Central Vietnam

Nguyen Anh Duong[1,3]* and Vu Van Chinh[2,4]

[1]Institute of Geophysics, Vietnam Academy of Science and Technology, 18 Hoang Quoc Viet, Cau Giay, Hanoi 11307, Vietnam
[2]Institute of Geological Sciences, Vietnam Academy of Science and Technology, 84 Chua Lang, Dong Da, Hanoi 11512, Vietnam
[3]Graduate University of Science and Technology, Vietnam Academy of Science and Technology, 18 Hoang Quoc Viet, Cau Giay, Hanoi 11307, Vietnam
[4]Vietnam Association of Tectonics, 84 Chua Lang, Dong Da, Hanoi 11512, Vietnam

ABSTRACT: We have applied geomorphology to investigate the tectonic fault in the North Central Vietnam. At the local scale, the active tectonic possibility of fault zones in the study area is geomorphologically assessed for the first time. The results show the geomorphic indices of drainage basin asymmetry (AF = 0–34), valley floor width-to-height ratio (V_f = 0.21–1.71) applied to 50 drainage basins and mountain-front sinuosity (S_{mf} = 1.07–1.58) calculated along 17 tectonic fault zones. The geomorphic analysis indicates that the modern activity of faults in the study area is moderate–weak. Only a few segments of the Truong Son and Dakrong-Hue faults are assessed as strongly active. The tectonic activity of this area is assessed with an average uplifting rate of about 0.2 mm/year according to the S_{mf} and V_f analyses. In order to prove the existence of faults as well as their active possibility, the field survey has also been carried out by structural geological and geomorphological methods. The survey was conducted at 369 outcrops and approximately 12,000 fractures were measured. Based on the data on displacement and the processing of data on slip observed at the outcrops, we have identified the strike-slip tectonic stress state of Pliocene–Quaternary period with the sub-longitudinal compressional direction and the slip mechanism of fault zones in this period. It is a new finding of the contemporary crustal stress orientation of North Central Vietnam. The results of this study provided the geomorphic evidence to evaluate the potential seismic hazards of the North Central Vietnam.

Key words: tectonic geomorphology, geomorphic indices, active tectonic fault, North Central Vietnam

Manuscript received June 15, 2020; Manuscript accepted February 21, 2021

1. INTRODUCTION

Landscape evolution is always the result of tectonic activity and surface processes (Bishop, 2007). In the studies of the active tectonic fault system, therefore, geomorphology has maintained a central position. Based on the calculation of geomorphic indices using topographic maps and field works, the quantitative measurement of the landscape is implemented (Keller and Pinter, 2002). The previous studies have proven that geomorphic indices have allowed calibrating the rates of the spatial distribution of deformation of tectonics. Continually, along with the development of the digital elevation model and geographic information system, the quantitative geomorphic indices have provided the capability to identify different structural segmentations along the active fault and the most likely active segment (Summerfield, 2000; Azor et al., 2002).

Because of the important effect of drainage basin formation and its dynamics, it has long been a major subject of study in geomorphology. The method applied to the study of the drainage basin is greatly sensitive to active faults and tectonics. Currently, the geomorphic indices, such as the ratio of valley floor width to valley height, mountain front sinuosity (Bull and McFadden, 1977), drainage basin asymmetry (Hare and Gardner, 1985), and so on, have been developed as quantitative tools to express the drainage basin characteristic and to analyze active tectonic fault.

The collision between the Indian-Australian plate and the Eurasian plate has resulted in the formation of the numerous strike-slip faults from Myanmar to the East Vietnam Sea in the early Cenozoic (Tapponnier et al., 1982; Lacassin et al., 1997; Morley, 2004; Yin, 2010). According to the research of Duong et al. (2013), the deformation boundary zone between South China block and Sundaland block is from Northwestern Vietnam to Central Vietnam where the deformation is accommodated by the NW-

*Corresponding author:
Nguyen Anh Duong
Institute of Geophysics, Vietnam Academy of Science and Technology, 18 Hoang Quoc Viet, Cau Giay, Hanoi 11307, Vietnam
Tel: +84-24-3756-4360, Fax: +84-24-3836-4696,
E-mail: duongna@igp-vast.vn

SE trending fault zones. Due to the long history of geological development, from Proterozoic up to now, the Earth's crust in North Central Vietnam has been broken by many fault systems in different directions and has been recorded on the maps of geology at scales 1:1,000,000 (Tien et al., 1991) and 1:200,000 (Trang et al., 1996); on the maps of earthquake disaster research (Xuyen and Thuy, 1996; Xuyen, 2004; Thuy, 2005, 2007); on the maps of soil cracking (Thom, 2002; Yem, 2005). The previous studies have only been exploiting the specific aspects of some major fault zones without analyzing and comprehending the detailed map of active faults for the whole region. The faults have been preliminarily studied and classified into modern active faults in Vietnam on a map with a small scale of 1:1,000,000 (Xuyen et al., 2004). Although, there are several studies on the tectonic faults (Thom, 2001; Xuyen, 2004; Minh, 2015), deep crustal structures (Hung et al., 2019) and seismic hazards for local areas (Phuong and Truyen, 2014; Duong et al., 2017), so far there is a lack of detailed studies on the active tectonic possibility of faults throughout the area of North Central Vietnam. Based on additional survey documents at 369 outcrops on the mainland of Vietnam with approximately 12,000 fractures measured, combined with satellite image interpretation and the above mentioned documents, we have built up a tectonic fault map for North Central Vietnam, where the location of the faults has been accurate from

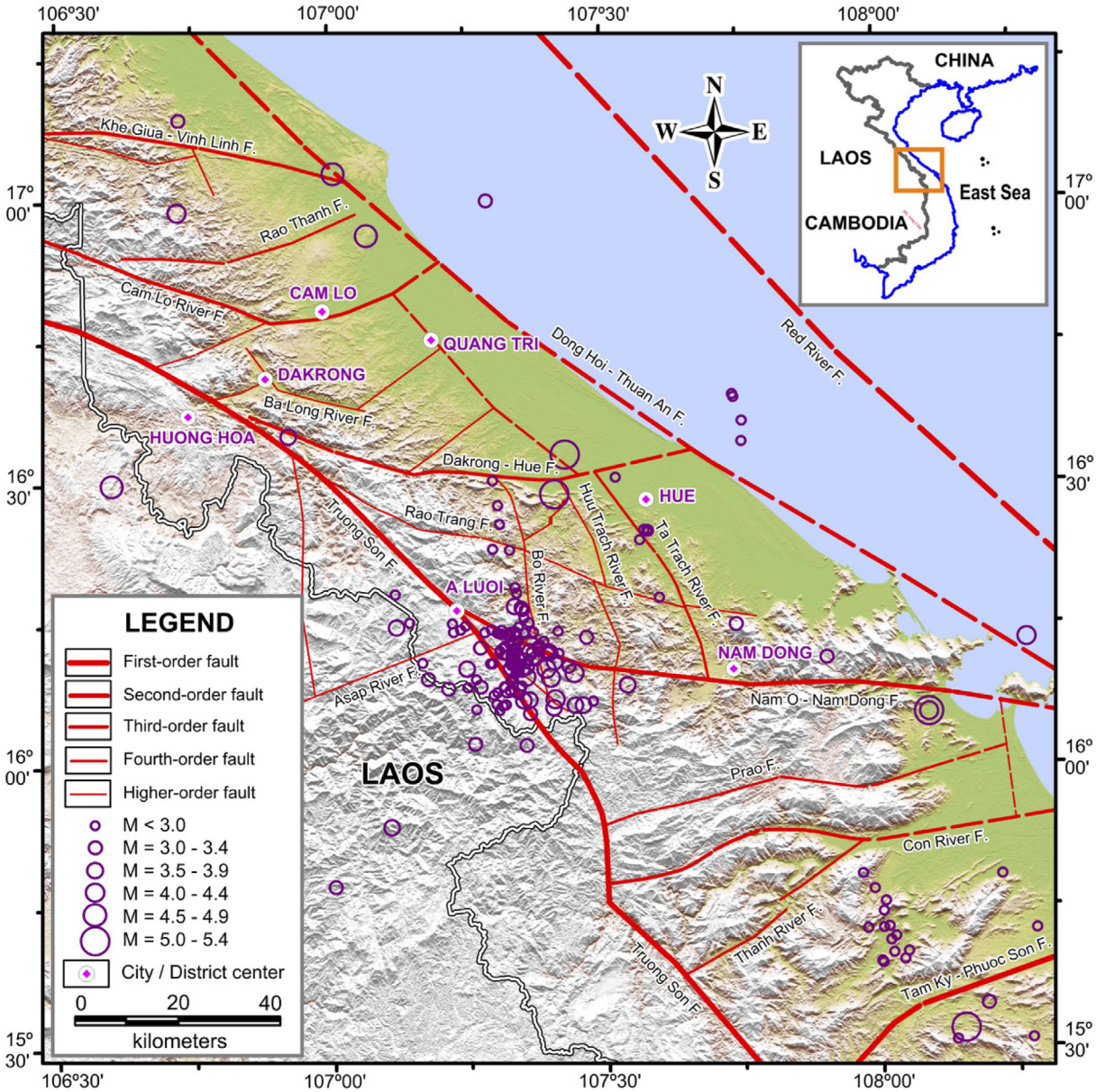

Fig. 1. Map of faults and earthquakes (M > 1.0) in the period 1666–2019 in the North Central Vietnam. Small box denotes the location of the study area in Vietnam. Topography uses the gradient calculated from SRTM (Shuttle Radar Topography Mission) data available at http://earthdata.nasa.gov.

the additional survey results (Fig. 1). The rupture of the rocks distributed in the two sides along the fault line has created favorable conditions for the active surface processes, especially the weathering and erosion processes. Most of the flows coincidentally develop on the tectonic fractures, especially large faults such as the Truong Son, the Nam O-Nam Dong, the Dakrong-Hue faults.

The North Central Vietnam is known as a region with moderate seismic activity in Vietnam. There were at least 215 earthquakes with a magnitude range of 1.0–5.1 that occurred from 1666 to July 2019 in the vicinity of the fault zones (Fig. 1). The probability of earthquake occurrence is high in a complicated geological structure, dominated by many tectonic faults, such as the Truong Son, the Dakrong-Hue and the Nam O-Nam Dong, Tam Ky-Phuoc Son faults (Fig. 1). There were five moderate earthquakes with a magnitude greater than 4.5 in the study area: the 1829 M5.1 and the 1947 M4.9 in Dakrong-Hue fault, the 1947 M5.1 in Nam O-Nam Dong fault, the 2014 M4.7 in Truong Son fault, and the 1715 M5.0 in Tam Ky-Phuoc Son fault.

In this work, the methods of drainage basin asymmetry, valley floor width to valley height ratio, and mountain front sinuosity

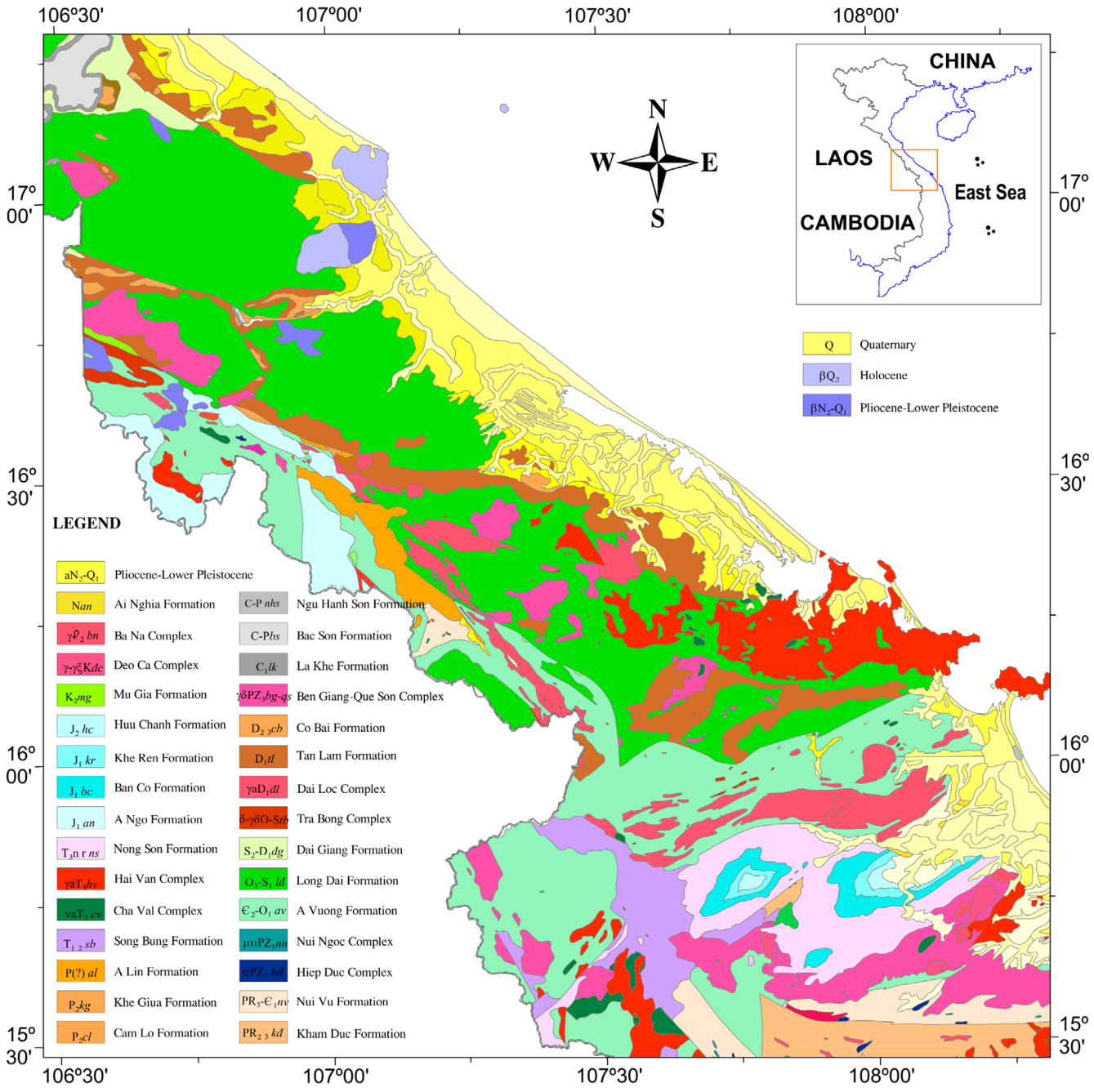

Fig. 2. Schematic geological map of North Central Vietnam (simplified from Trang et al., 1996).

https://doi.org/10.1007/s12303-021-0006-6

have been applied and commonly analyzed in modern tectonic studies in the North Central Vietnam. Such analyses have been used widely and successfully in the investigation of the modern tectonic activity of different areas such as in America, Iran, Spain, Italy, and Turkey (e.g., El Hamdouni et al., 2008; Bagha et al., 2014; Troiani et al., 2014; Yildirim, 2014; Pavano et al., 2016). For the North Central Vietnam area, this is the first study to investigate the geomorphology and active tectonic fault in detail. The result of activity of tectonic fault zones will be an essential information for the seismic hazard analysis in the study area.

2. GEOLOGICAL AND SEISMOTECTONIC SETTINGS

In the North Central Vietnam, the geological platform of the southwestern and southern parts belongs to Indosinian geoblock, that of the central part belongs to Truong Son fold system and that of the northeast part belongs to Red River basin (Trang et al., 1996). The strata of the study area include Late Proterozoic–Early Paleozoic metamorphic sedimentary rocks, Paleozoic sedimentary rocks, Neogene terrigenous sediments, and Quaternary unconsolidated sediments. They belong to the following formations (Fig. 2):

– Nui Vu formation of Late Proterozoic–Cambrian age (PR_3–$\varepsilon_1$nv) has the relatively narrow distribution area in the southwest near the Laos border. This formation consists of plagioclase-amphibole schist, actinolite-chlorite-epidote schist, quartz-mica schist, quartz-sericite schist, and cherty schist.

– A Vuong formation of Cambrian–Ordovician age ($\in_2$–O_1av) is also mainly distributed in the southwest of the study area. The lower part of the formation consists of sericite-quartz schist, mica schist, sericite-chlorite schist interbedded with shale, greenstone lenses, and quartzitic sandstone. The middle part is composed of quartzitic sandstone interbedded with quartz-sericite-chlorite schist, shale, and marbleized limestone lenses. The upper part is comprised of sericite-quartz schist, sericite-chlorite schist, quartzitic sandstone, marl lenses, and locally interbedded with actinolite-zoisite-epidote schist.

– Long Dai formation of Ordovician–Silurian age (O_3–S_1ld) consists of rhythmic quartzitic siltstone and sandstone interbedded with andesite, shale intercalated with siltstone, silty sandstone interbedded with rhythmic chlorite shale, shale and siltstone intercalated with cherty shale, quartzitic sandstone interbedded with shale, chlorite shale interbedded with quartzitic sandstone, gritstone and tuff. The rocks of Long Dai formation account for the majority of the study area.

– Tan Lam formation of Early Devonian age (D_1tl) is distributed into a narrow strip in the northwest-southeast direction in the southwest of Hue city. The rocks of Tan Lam formation are comprised of limestone, marl interbedded with shale, massive limestone, bedded limestone and locally stripped limestone.

– Co Bai formation of Middle–Late Devonian age (D_{2-3}cb) has the extremely limited distribution area, often associated with the rocks of Tan Lam formation.

– A Lin formation consists of two parts. The lower part is composed of andesitic tuff; pebble-bearing gritstone interbedded with siltstone; andesite; siltstone; andesite, andesitic tuff; porphyritic dacite; siltstone intercalated with andesitic tuffaceous conglomerate. The upper part is comprised of clayish limestone, siltstone; tuffaceous gritstone; polymictic sandstone; sandstone, polymictic gritstone; conglomerate interbedded with sandstone; siltstone, polymictic sandstone intercalated with tuffaceous sandstone; pebble-bearing gritstone; silty sandstone; tuffaceous conglomerate. The age of the formation has not yet been clearly determined and is temporarily classified in Permian (P(?)al).

– Pliocene–Lower Pleistocene sediment (N_2–Q_1) consists of pebble, breccia, grit, sand and clay. They have a limited distribution area along the Ta Trach River.

– Quaternary unconsolidated sediment is composed of pebble, breccia, sand, silt, mainly distributed in the northeast along the coast and in narrow areas along rivers and streams.

The fault system in the study area was recorded with tectonic activity in the Pliocene–Quaternary. These faults have been established based on geological data, results of remote sensing image interpretation, field surveys of structural geology, processing of gravity and magnetic data. The tectonic faults develop in different directions, the majority in the northwest-southeast, sub-latitudinal, sub-longitudinal directions and the minority in the northeast-southwest direction (Fig. 1). The Truong Son fault (first-order fault) follows the northwest-southeast direction and runs through the southwestern part of the study area in A Luoi district. The fault dips quite steeply towards the northeast with an angle of 70–80°. The Nam O-Nam Dong fault (second-order fault) is a branch fault of the Truong Son fault, with the northwest-southeast direction in the west and the sub-latitudinal direction in the east. The northwest-southeast segment (the western part) dips vertically, meanwhile, the sub-latitudinal segment (the eastern part) dips steeply towards the south with an angle of 70–80°. The Dakrong-Hue fault (third-order fault) follows the sub-latitudinal direction, runs through Hue city and extends seawards. The Dakrong-Hue fault dips towards the north-northeast with an angle of 65–70°. The fourth-order and higher-order faults consist of a series of faults such as Ta Trach River, Rao Trang, Bo River, Huu Trach in different directions.

3. METHODOLOGY

In this study, geomorphic indices such as drainage basin

asymmetry (AF) (Hare and Gardner, 1985), mountain front sinuosity (S_{mf}) and valley floor width-to-height ratio (V_f) (Bull and McFadden, 1977) are used to assess the activity of fault zones in the study area.

3.1. Drainage Basin Asymmetry (AF)

There are two causes of drainage basin asymmetry: the different lithological characteristics between two halves of drainage basin or/and the unequal tectonic movement between two halves of basin. Therefore, the drainage basin asymmetry can help to determine the formation as well as the tectonic state of the basin. The asymmetry factor $AF = (A_r/A_T) \times 100$ is one of the indices used to assess the tectonic inclination of the basin (Hare and Gardner, 1985; Cox, 1994; Keller and Pinter, 2002), in which A_r is the remaining area on the right of the flow direction and A_T is the total drainage area of the basin.

It can be seen that in symmetric basins, the AF value is approximately 50, the inclination perpendicular to the main flow direction is less than or equal to 0 (Mahmood and Gloaguen, 2012). In asymmetric basins, the AF value is significantly larger or smaller than 50. This indicates that the influence of active tectonics or different erosion factors causes the varied inclinations of the basin (Hare and Gardner, 1985; Keller and Pinter, 2002; Scotti et al., 2014). The AF values can be divided into three main groups as follows: $45 < AF < 55$ (symmetric basin), $AF > 55$ (asymmetric eastward basin) and $AF < 45$ (asymmetric westward basin) (Ozkaymak and Sozbilir, 2012). Meanwhile, Perez-Pena et al. (2010) used the measurement scale: $AF = |(A_r/A_T) \times 100 - 50|$. According to this scale, $AF < 5$, $AF = 5–10$, $AF = 10–15$ and $AF > 15$ correspond to the symmetric, slightly asymmetric, moderately asymmetric and non-symmetric basins, respectively.

3.2. Valley Floor Width-to-Height Ratio (V_f)

Another geomorphic index that can be used to assess the tectonic activity in the area is the valley floor width-to-height ratio (V_f). The ratio $V_f = 2V_{fw}/[(E_{ld} - E_{sc}) + (E_{rd} - E_{sc})]$ reflects the shape of cross-section of the valley and the formation time of the valley (Keller and Pinter, 2002), in which V_{fw} is the width of the valley floor; E_{ld} and E_{rd} are the elevations of the left and right valley divides, respectively; E_{sc} is the elevation of the valley floor.

The greater the tectonic uplifting movement, the deeper and narrower the valley with "V" shape, and the V_f value is small. In contrast, the high V_f values correspond to the valleys which have a wide floor, "U" shape, and relatively slight tectonic activity (Bull and McFadden, 1977; Rockwell et al., 1984; Silva et al., 2003; Perez-Pena et al., 2010).

In small river valleys, the cross-section of the valley is used to determine V_f at approximately 250 m towards the mountain front. In large drainage basins, the cross-sections of the valleys are defined at about 250 m and 500 m upstream of the mountain front (Bull, 1977; Ramirez-Herrera, 1998; Tsodoulos et al., 2008; Ozkaymak and Sozbilir, 2012).

3.3. Mountain Front Sinuosity (S_{mf})

The mountain front sinuosity (S_{mf}) reflects the correlation between flow erosion and tectonic uplifting movement, and is determined by $S_{mf} = L_{mf}/Ls$ (Bull and Fadden, 1977), in which L_{mf} is the total length of the lowest contour line of the mountain front and L_s is the straight-line length of the mountain front.

If the geological platform of the area is homogeneous, the S_{mf} reflects the rate of uplifting movement. When the uplifting movement prevails, the mountain front is relatively straight, corresponding to the small L_{mf} value. However, if the uplifting slows down or stops and the erosion starts, the mountain front will become more sinuous and wider, the L_{mf} value is great. According to the analytical studies on the mountain front sinuosity, if the S_{mf} value is low (1–1.5), the mountain front is considered as the active front (Malik and Mohanty, 2007). If the S_{mf} value is greater than 3, the mountain front is mainly affected by the erosion (Bull and Fadden, 1977; Rockwell et al., 1984; Wells et al., 1988; Silva et al., 2003).

4. DATA

Based on the digital topographic map at a scale of 1:50,000, the fault map and field survey data, we have determined 50 drainage basins (Fig. 3). The main flows of selected drainage basins coincide or nearly coincide with the faults. Normally, the right and left basins of the flow are determined according to the flow direction. However, in order to synchronize with the input data and facilitate the assessment of activity and movement of faults in the study area according to AF indices, the right and left banks of basins are defined as follows: the area of drainage basin located on the left of the fault is the left bank and that located on the right of the fault is the right bank.

In the study area, the V_f values are determined on 69 cross-sections. In order to ensure that the cross-sections are perpendicular both to the river flow and to the strike of the assessed fault zone, the cross-sections were selected at the locations where the fault zone coincides or nearly coincides with the main river flow. In case of the fault zones with many cross-sections, the cross-sections are arranged as follows: from the northwest to the southeast for the northwest-southeast, west northwest-east southeast or north northwest-south southeast fault zones; from the southwest to the northeast for the northeast-southwest fault

https://doi.org/10.1007/s12303-021-0006-6

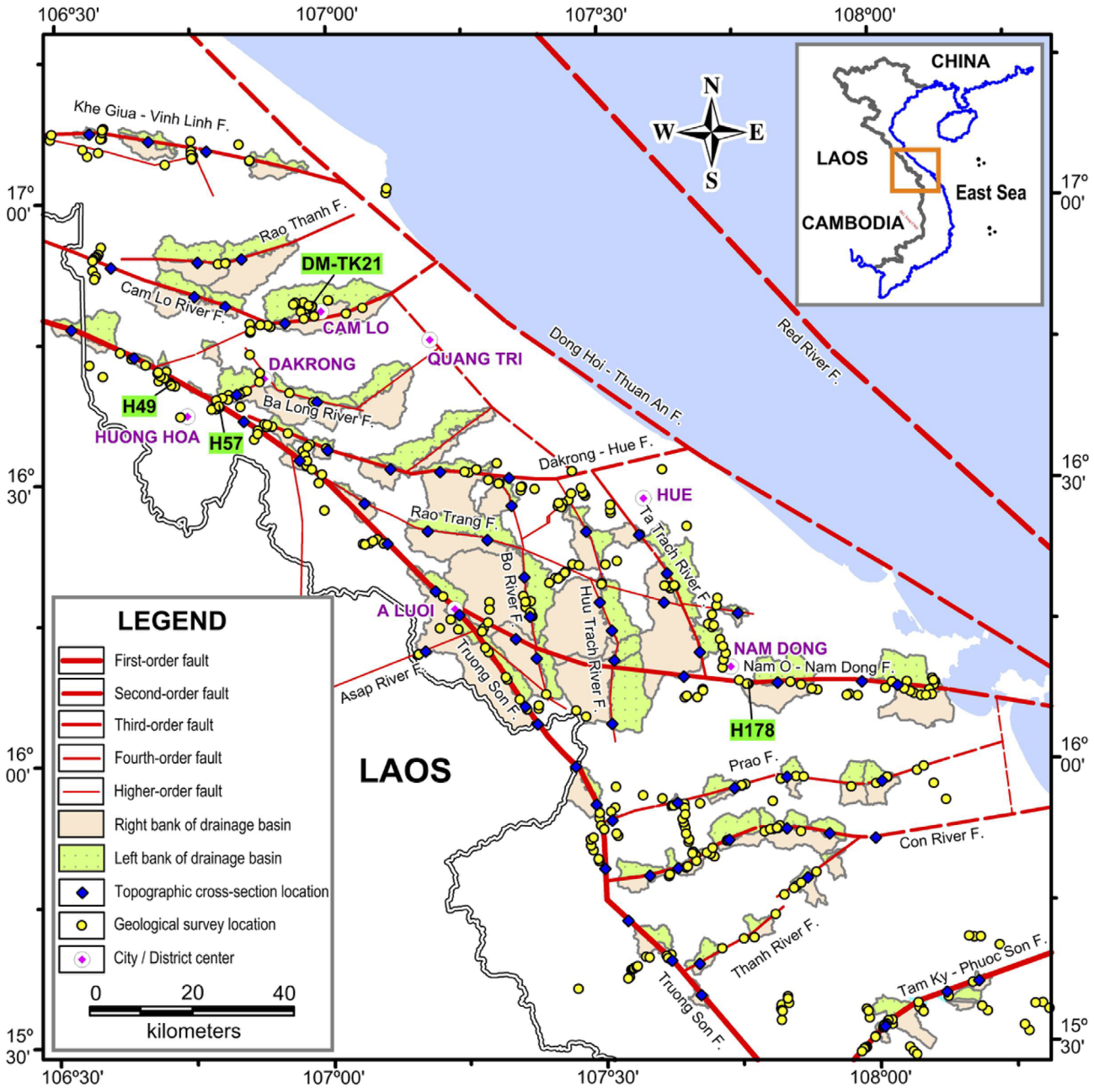

Fig. 3. Map of drainage basins, topographic cross-section locations and geological survey sites in the North Central Vietnam. Some descriptions are the same as Figure 1.

zones; and from the west to the east for the latitudinal or sub-latitudinal fault zones. The locations of topographic cross-sections in the study area are shown in Figure 3. The examples of topographic cross-sections running through the Truong Son fault zone are presented in Figure 4. Accordingly, 15 cross-sections perpendicular to the segments of Truong Son fault zone are numbered as follows: TS1, TS1a, TS2, TS2a, TS3, TS4, TS4a, TS5, TS5a, TS5b, TS6, TS6a, TS7, TS7a and TS8, in which the TS1 and TS1a cross-sections are located in the northwest and perpendicular to the TS01 fault segment, meanwhile the TS8 cross-section is located in the southeast and perpendicular to the TS08 segment.

In this study, the S_{mf} index is calculated from the digital topographic map of the study area at a scale of 1:50,000. The mountain fronts or the selected foot-slope lines (the lowest contour lines) have the common strike relatively parallel to the assessed fault segment and develop in the area with a homogeneous geological platform. The river and stream segments whose flows coincide or nearly coincide with the faults have been selected. In the study area, there are 56 flow segments that meet these criteria.

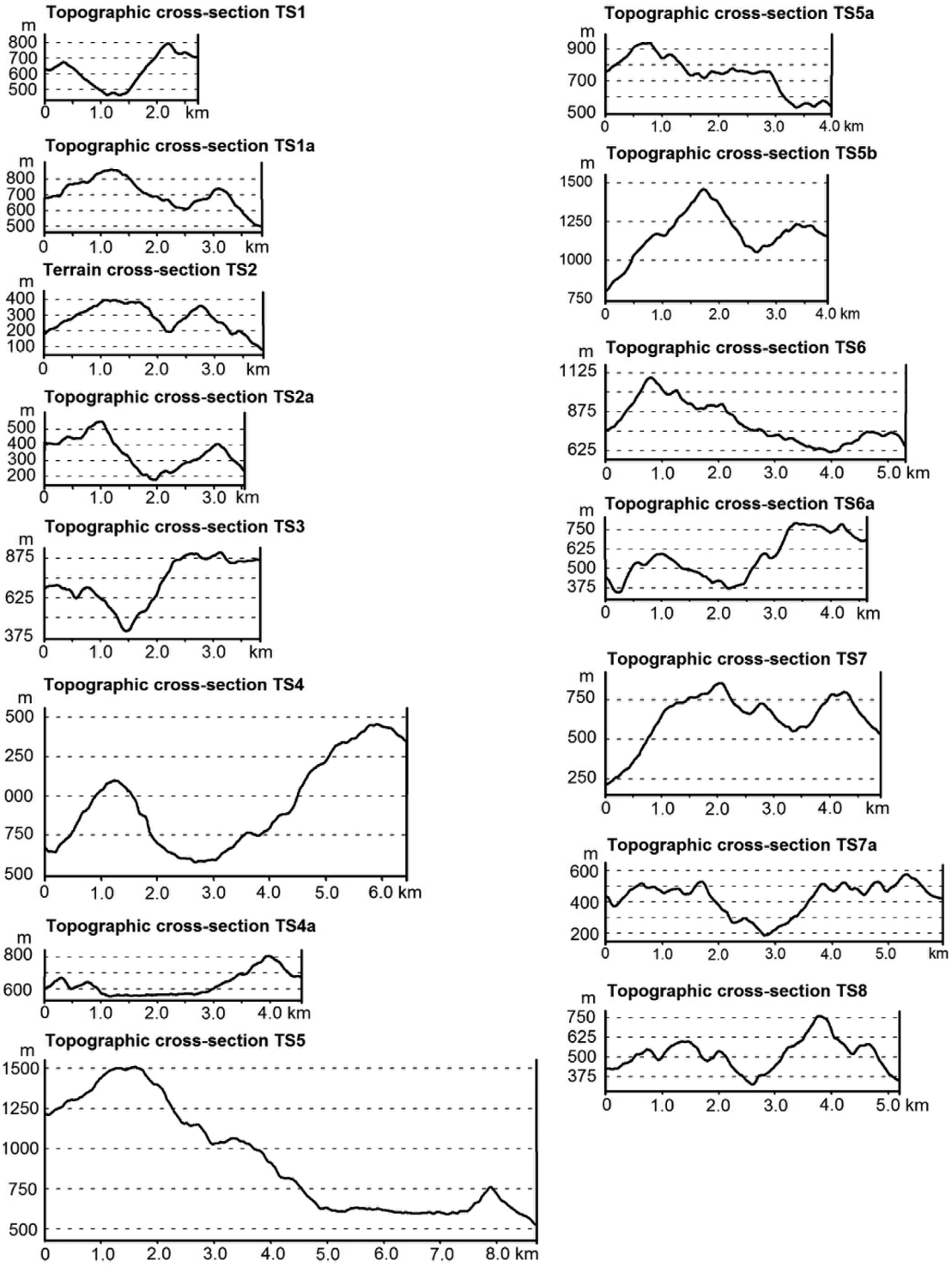

Fig. 4. Some examples of topographic cross-sections running through the Truong Son fault zone.

5. RESULTS AND DISCUSSION

5.1. Drainage Basin Asymmetry (AF)

The asymmetry factor AF according to the formula of Perez-Pena et al. (2010) is used in this study, ranging from 0 to 34 (Table 1). Accordingly, 22% of AF values reflect the symmetric basins in the area, and 78% reflects the asymmetric basins. The average value and standard deviation of AF are 14.0 and 7.0, respectively. With such average value and standard deviation, the AF values for asymmetric basins in the study area are divided into three ranges: 5.0–7.0, 7.0–21.0, and > 21.0. These AF ranges,

https://doi.org/10.1007/s12303-021-0006-6

respectively, correspond to the activity levels of relevant fault segments: weak (level 3), moderate (level 2), and strong (level 1). For asymmetric basins, these AF values are determined as follows: 15% slightly asymmetric, 55% moderately asymmetric, and 30% completely asymmetric.

The activity of fault zones in the study area is mostly moderate and weak according to the AF. The strongly active fault segments mainly belong to higher-order fault zones, such as Bo River and Rao Trang fault zones. There are also some strongly active segments on the third-order fault zones, such as DR-H02, DR-H03 of Dakrong-Hue fault zone, SC02 of Con River fault, however, none of these segments belong to the first-order Truong Son and Tam Ky-Phuoc Son fault zones and the second-order Nam O-Nam Dong fault zone.

5.2. Valley Floor Width-to-Height Ratio (V_f)

The parameters and results of the calculation of valley floor width-to-height ratio in the North Central Vietnam are presented in Table 1. The average V_f value ranges from 0.21 to 1.71, with most V-shaped valleys changing to U-shaped ones. The average value and standard deviation of V_f are 0.43 and 0.19 respectively. Consequently, the V_f values are divided into three ranges: < 0.24, 0.24–0.62 and > 0.62, which correspond to the activity levels of fault segment where the cross-section cuts through: strong (level 1), moderate (level 2), and weak (level 3). Accordingly, 12% of V_f values is less than 0.24; 53% of V_f values is between 0.24–0.62, and 35% of V_f values is greater than 0.62.

The V_f value indicates that the activity of fault zones in the study area is mainly moderate and weak. However, there are some fault zones with strongly active segments, for example, TS02, TS03, TS05, TS06 and TS07 of the first-order Truong Son fault zone; KG-VL01 of the third-order Khe Giua-Vinh Linh fault zone; DR-H02 of the third-order Dakrong-Hue fault zone; SC01, SC02, SC03 of the third-order Con River fault zone; and SB01 of the higher-order Bo River fault zone.

5.3. Mountain Front Sinuosity (S_{mf})

The calculation results show that the S_{mf} index varies from 1.07 to 1.58 along 17 tectonic fault zones in the North Central Vietnam. The average value and standard deviation of S_{mf} are 1.31 and 0.1 respectively. Consequently, the S_{mf} values have been divided into three ranges: low (< 1.21), moderate (1.21–1.41), and high (> 1.41). These three ranges of S_{mf} can be considered to correspond to the development stages of river and stream valleys: young, mature, and old. In the young stage, the valley is formed mainly by the deep erosion; in the mature stage, both deep and horizontal erosions play an important role in the formation of the valley; in the old stage, the valley develops with the dominance of horizontal erosion and accumulation. Three ranges of S_{mf} correspond to three activity levels of fault zone: strong (level 1), moderate (level 2), and weak or inactive (level 3). In the study area, 18% of S_{mf} values are less than 1.21, 70% of S_{mf} values are in the range of 1.21–1.41, and 12% of S_{mf} values are greater than 1.41. It can be clearly seen from the S_{mf} values that the activity of fault zones in the study area is mainly moderate. However, there are also some strongly active segments, such as TS07 of the first-order Truong Son fault zone; KG-VL01 of the third-order Khe Giua-Vinh Linh fault zone; DR-H01, DR-H02, DR-H03 of the third-order Dakrong-Hue fault zone; SC01 of the third-order Con River fault zone.

5.4. Assessment of Activity of Fault Zones According to Geomorphic Indices

The activity of fault zones in the North Central Vietnam is assessed as strong, moderate and weak, corresponding to three levels 1, 2 and 3, respectively. The comparison of the ranges of geomorphic indices AF, V_f and S_{mf} in the study area reveals the similarity with the ranges of geomorphic indices divided for other regions in the world (e.g., Dehbozorgi et al., 2010; Giaconia et al., 2012; Mahmood and Gloaguen, 2012; Sharma et al., 2018).

The overall assessment of the activity of fault segments in fault zones in the study area is simultaneously conducted according to three geomorphic indices AF, V_f and S_{mf}. The fault segment is assessed as strongly active when all three indices AF, V_f and S_{mf} on this segment are at level 1, or two of the three indices are at level 1 and the remaining index is at level 2; it is assessed as moderately active when all three geomorphic indices are at level 2; and it is assessed as weakly active when all three indices are at level 3, or two of the three indices are at level 3 and the rest is at level 2. In addition, there are intermediate levels: averagely strong and averagely weak. The activity of fault segment is assessed as averagely strong when two of three indices on this segment are at level 2 and the remaining index is at level 1; it is assessed as averagely weak when two of three indices are at level 2 and the rest is at level 3.

According to the above assessment, among 55 fault segments, only 5 segments are considered to be strongly active, in which only 1 segment is located in the third-order Dakrong-Hue fault zone (segment DR-H02), the rest belong to the higher-order fault zones. 11 segments are assessed as averagely strong; 19 segments – moderate; 13 segments – averagely weak and 7 segments – weak (Table 2). The result of this assessment indicates that the modern activity of fault zones in the study area is mainly moderate and weak, the number of strong and averagely strong segments is not considerable.

Table 1. Geomorphic indices in the North Central Vietnam

Fault	Segment of fault	$AF^{(a)}$	$AF^{(b)}$	V_f	$V_f^{(c)}$	sigma	S_{mf}
Truong Son	TS01	33	17	0.27	0.81	1.41	1.35
	TS01a			0.67			
	TS02	64	14	0.18			
	TS02a			0.27			
	TS03	49	1	0.14			
	TS04	67	17	0.5			
	TS04a			4.41			
	TS05	67	17	4.1			
	TS05a			0.16			
	TS05b			0.14			
	TS06	71	21	0.29			
	TS06a			0.22			
	TS07	48	2	0.18			
	TS07a			0.24			
	TS08	63	13	0.39			
Tam Ky - Phuoc Son	TK-PS01	62	12	1.89	1.71	0.92	1.28
	TK-PS02	70	20	3.27			
	TK-PS02a			1.53			
Nam O - Nam Dong	NO-ND01	69	19	0.28	0.34	0.87	1.31
	NO-ND02	37	13	0.47			
	NO-ND03	46	4	0.29			
	NO-ND04	53	3	0.31			
	NO-ND05			2.27			
Khe Giua - Vinh Linh	KG-VL01	47	3	0.17	0.58	0.65	1.33
	KG-VL02	59	9	0.24			
	KG-VL03	55	5	1.33			
Cam Lo River	SCL01	58	8	0.35	0.51	0.22	1.40
	SCL02	44	6	0.58			
	SCL03	44	6	0.31			
	SCL04			0.78			
Dakrong - Hue	DR-H01	51	1	0.4	0.42	0.17	1.13
	DR-H01a			0.42			
	DR-H02	76	26	0.22			
	DR-H03	82	32	0.63			
Con River	SC01	52	2	0.37	1.30	1.68	1.36
	SC01a			0.12			
	SC02	28	22	0.14			
	SC03	55	5	0.22			
	SC03a			3.43			
	SC04			3.51			
Rao Thanh	RTh01	48	2	0.24	0.18	0.08	1.58
	RTh02	66	16	0.12			
Ta Trach River	STT01	49	1	2.5	1.71	1.54	1.40
	STT02	67	17	4			
	STT02a			0.92			
Prao	PR01	59	9	0.88	0.56	0.31	1.29
	PR02			0.71			
	PR02a	31	19	0.68			
	PR03	50	0	0.46			
	PR04	58	8	0.08			

https://doi.org/10.1007/s12303-021-0006-6

Table 1. (continued)

Fault	Segment of fault	AF[(a)]	AF[(b)]	V_f	V_f[(c)]	sigma	S_{mf}
Thanh River	ST01	40	10	0.46	0.52	0.08	1.24
	ST02	74	24	0.57			
Dakrong	DR01	42	8	0.88	0.88	0	1.07
Ba Long River	SBL	73	23	0.32	0.32	0	1.07
Bo River	SB01	80	30	0.15	0.24	0.09	1.37
	SB02	77	27	0.22			
	SB02a			0.22			
	SB03	72	22	0.37			
Huu Trach River	SHT01	58	8	4.16	1.16	1.69	1.45
	SHT02	78	28	0.4			
	SHT02a			0.27			
	SHT03	31	19	0.77			
	SHT04	55	5	0.19			
Rao Trang	RT01	78	28	0.63	0.37	0.29	1.32
	RT02	52	2	0.04			
	RT03	84	34	0.17			
	RT04	77	27	0.7			
	RT05	68	18	0.29			
A Sap River	SAS			0.21	0.21	0	1.32

AF determined by using the formulas of Hare and Gardner (1985)[(a)], Perez-Pena et al. (2010)[(b)], averaged V_f value[(c)]; sigma: standard deviation of V_f.

Table 2. Assessment of the activity on the segments of fault zones in the North Central Vietnam according to geomorphic indices AF, V_f and S_{mf}: (1) strongly active; (2) moderately active; (3) weakly active

Fault	Segment of fault	Tectonic level			Assessment of active tectonic level
		AF	V_f	S_{mf}	
Truong Son	TS01	2	2	2	Moderate
	TS02	2	1	2	Moderate–strong
	TS03	3	1	2	Moderate
	TS04	2	2	2	Moderate
	TS05	2	1	2	Moderate–strong
	TS06	2	1	3	Moderate
	TS07	3	1	1	Moderate–strong
	TS08	2	2	2	Moderate
Tam Ky-Phuoc Son	TK-PS01	2	3	2	Moderate–weak
	TK-PS02	2	3	2	Moderate–weak
Nam O-Nam Dong	NO-ND01	2	2	2	Moderate
	NO-ND02	2	2	2	Moderate
	NO-ND03	3	2	2	Moderate–weak
	NO-ND04	3	2	2	Moderate–weak
	NO-ND05	–	3	2	Moderate–weak
Khe Giua-Vinh Linh	KG-VL01	3	1	1	Moderate–strong
	KG-VL02	2	2	2	Moderate
	KG-VL03	3	3	3	Weak
Cam Lo River	SCL01	2	2	3	Moderate–weak
	SCL02	3	2	3	Weak
	SCL03	3	2	2	Moderate–weak
	SCL04	–	3	–	Weak
Dakrong-Hue	DR-H01	3	2	1	Moderate
	DR-H02	1	1	1	Strong
	DR-H03	1	3	1	Moderate–strong

Table 2. (continued)

Fault	Segment of fault	Tectonic level			Assessment of active tectonic level
		AF	V_f	S_{mf}	
Con River	SC01	3	1	1	Moderate–strong
	SC02	1	1	3	Moderate–strong
	SC03	3	2	3	Weak
	SC04	–	3	2	Moderate–weak
Rao Thanh	RTh01	3	2	2	Moderate–weak
	RTh02	2	1	3	Moderate
Ta Trach River	STT01	3	3	2	Weak
	STT02	2	3	3	Weak
Prao	PR01	2	3	2	Moderate–weak
	PR02	2	3	2	Moderate–weak
	PR03	3	2	2	Moderate–weak
	PR04	2	1	2	Moderate–strong
Thanh River	ST01	2	2	2	Moderate
	ST02	1	2	2	Moderate–strong
Dakrong	ĐR01	2	3	1	Moderate
Ba Long River	SBL	1	2	1	Strong
Bo River	SB01	1	1	2	Strong
	SB02	1	1	2	Strong
	SB03	1	2	2	Moderate–strong
Huu Trach River	SHT01	2	3	3	Weak
	SHT02	1	2	3	Moderate
	SHT03	2	2	3	Moderate–weak
	SHT04	3	1	2	Moderate
Rao Trang	RT01	1	3	2	Moderate
	RT02	3	1	2	Moderate
	RT03	1	1	2	Strong
	RT04	1	3	2	Moderate
	RT05	2	2	2	Moderate
A Sap River	SAS01	–	1	2	Moderate–strong

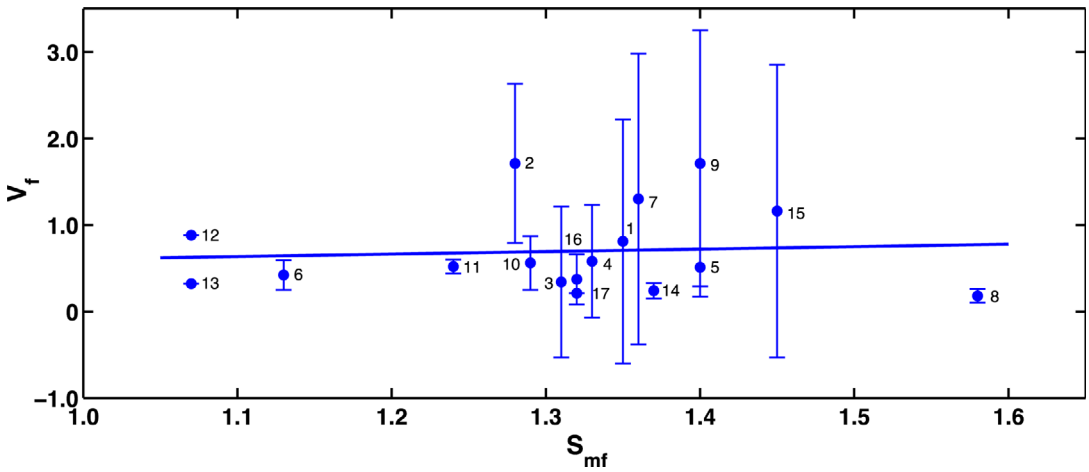

Fig. 5. Plot of S_{mf} vs. V_f for the mountain fronts of fauts in the North Central Vietnam. Vertical bars show the standard deviation of V_f values. Number at the right indicates the order of faults in Table 1.

Additionally, we can classify the tectonic activity of the study area based on the assessment of correlation between S_{mf} and V_f (Bull and McFadden, 1977). Figure 5 demonstrates the relationship between S_{mf} and V_f. Based on the simultaneous analysis of S_{mf} and V_f, the rate of uplifting movement in the study area can be determined. The uplifting rate of the study area is estimated at

https://doi.org/10.1007/s12303-021-0006-6

approximately 0.2 mm/year, this result is compared to the regression method with an accuracy of 52%. This is consistent with the uplift trending of the study area (Husson et al., 2018).

The earthquake activity in the study area is closely related to the neotectonic structural setting. Earthquakes are distributed into clusters and closely associated with active faults in the study area. The epicenter clusters are all located at the end of fault segments where the faults meet or intersect (Fig. 1). The study result shows that the level of expression of fault activity (moderate, generally) is consistent with the moderate earthquake activity in the region. The Dakrong-Hue fault zone is assessed as strongly active, it is in correspondence with two moderate earthquakes occurred (M = 5.1 in 1829 and M = 4.9 in 1947). Moreover, our study result is consistent with that of Xuan et al. (2020) on the level of expression of fault activity assessed by Radon activity index in soil gas, which is calculated by the ratio of anomaly value to background value of Radon concentration. The study result of Xuan et al. (2020) indicated that the Dakrong-Hue fault shows a strong expression of activity with very high Radon activity index.

Reservoir-induced seismicity in A Luoi district began to increase in 2012 after filling of the A Luoi hydropower reservoir. In particular, on May 15, 2014, in the area of A Luoi district, where the Truong Son and Nam O-Nam Dong faults intersect, an earthquake with magnitude M = 4.7 occurred (Fig. 1). The occurrence of earthquakes in the study area shows that the fault zones here have the potential to accumulate energy and show activity in the modern period, although the level of activity is moderate.

6. FIELD SURVEY

In order to prove the existence of faults as well as their active possibility in the North Central Vietnam, the field survey has been carried out by structural geological and geomorphological methods. The study area is about 40,000 km^2, in which 18,491 km^2 is the mainland of Vietnam, 11,870 km^2 belongs to the East Vietnam Sea, and 9,639 km^2 belongs to the territory of Laos. The survey was conducted at 369 outcrops on the mainland of Vietnam (Fig. 3) and 12,000 fractures were measured. In many outcrops, the destruction zones of the faults have been found. Some examples are presented in Figure 6.

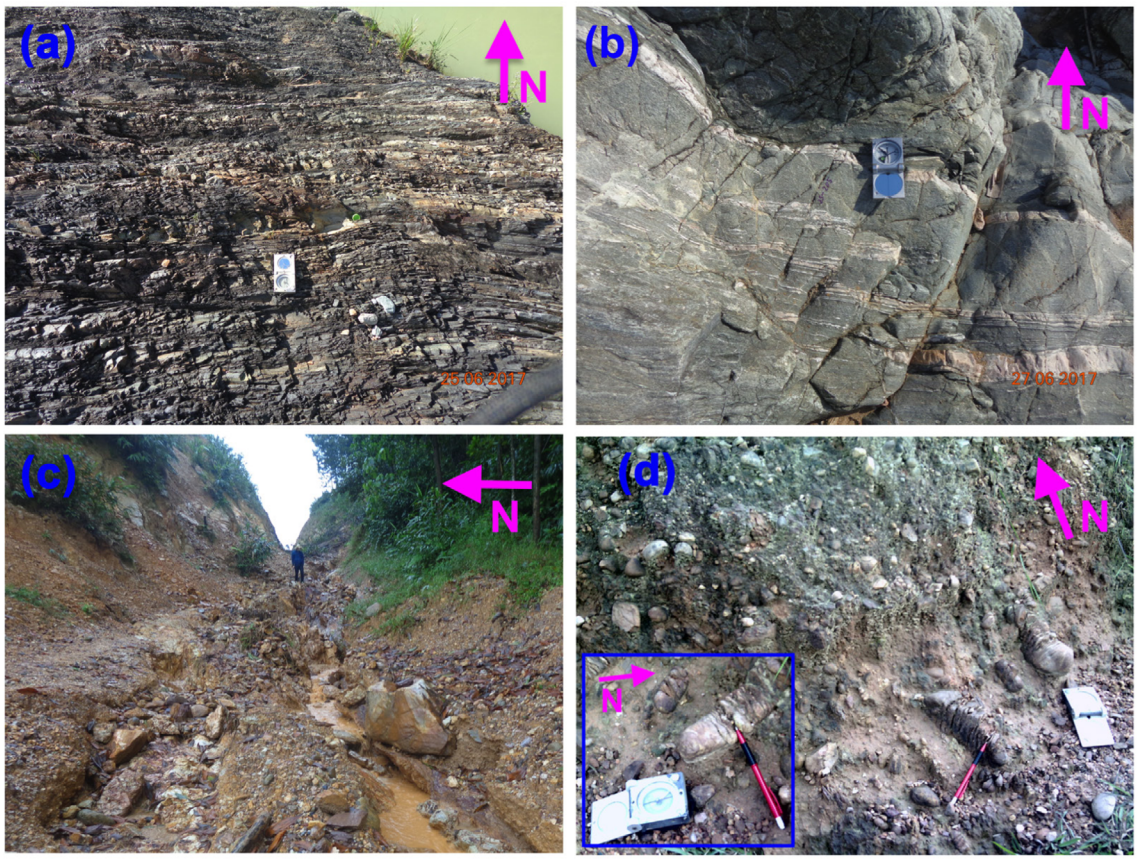

Fig. 6. Some examples of the destruction zones of faults at outcrops: (a) Outcrop H49 in Huong Tan commune, Huong Hoa district, Quang Tri province; (b) Outcrop H57 in Dakrong commune, Dakrong district, Quang Tri province; (c) Outcrop H178 in Huong Loc commune, Nam Dong district, Thua Thien Hue province; (d) Outcrop DM-TK21 in Tan Hiep village, Cam Tuyen commune, Cam Lo district, Quang Tri province. Their locations are showed in Figure 3.

Table 3. Characteristics of the tectonic stress state and the kinematics of the faults according to the slip surface – striation data in the North Central Vietnam

Outcrop No.	Coordinates		Attitude of slip surface (azimuth of dip direction/dip angle)	Attitude of striation (azimuth of dip direction/dip angle)	Movement direction	Principal stress vector (azimuth of stress axis/inclination of stress axis) (degree)		
	Latitude (degree)	Longitude (degree)				σ_1	σ_2	σ_3
Strike-slip fault with sub-longitudinal compressional direction								
RQ04	16.655	106.816	120/80	208/10	Sinistral	344/0	75/76	254/14
RQ07	16.638	106.794	138/85	228/5	Sinistral	3/0	93/83	273/7
RQ14	16.535	106.959	50/80	326/30	Dextral	11/14	124/58	274/29
RQ32	16.397	107.075	145/80	57/12	Sinistral	11/16	196/74	101/1
DM62	15.486	107.964	230/86	318/32	Dextral	9/25	146/58	269/19
DM22	15.659	107.610	215/85	125/5	Dextral	350/0	260/83	80/7
DM74	15.563	108.071	30/72	310/28	Dextral	352/7	92/55	257/34
H06	17.117	106.493	220/75	125/5	Dextral	355/7	239/74	87/14
H06	17.117	106.493	30/90	122/6	Dextral	165/4	301/84	75/4
H27	16.782	106.896	230/73	325/14	Dextral	2/22	190/68	93/2
H41	16.884	106.570	35/75	115/22	Dextral normal	168/26	338/64	76/4
H69	16.290	107.370	130/82	220/23	Sinistral	171/10	58/66	265/22
H157	16.491	107.465	65/60	335/8	Dextral	193/27	46/59	291/14
H183	16.141	108.107	215/86	120/25	Dextral	174 14	296/65	78/20
H184	16.139	108.111	45/70	125/10	Dextral	177/21	18/68	270/7
H184	16.139	108.111	30/80	130/15	Dextral	164/18	333/72	73/3
H184	16.139	108.111	45/80	125/25	Normal	180/25	335/63	86/10
H184	16.139	108.111	225/86	310/5	Dextral	360/6	174/84	270/1
H184	16.139	108.111	210/75	315/10	Dextral	343/18	176/72	74/4
H188	16.119	108.072	40/80	310/10	Dextral	176/0	85/76	266/14
Normal - strike-slip fault with sub-latitudinal extensional direction								
H99	15.943	107.572	145/75	70/30	Sinistral	11/32	211/57	107/9
H109	15.849	107.698	290/60	270/50	Normal	163/55	357/34	263/7
H185	16.134	108.108	70/60	140 30	Dextral normal	195/41	21/49	288/3
Reverse fault, reverse - strike-slip fault with sub-longitudinal compressional direction								
H01	17.118	106.587	340/55	56/28	Reverse	199/8	297/46	102/43
H50	16.562	106.954	135/40	135/40	Reverse	349/14	87/29	236/56
H54	16.605	106.896	196/78	196/78	Reverse	186/32	283/12	31/55
H54	16.605	106.896	195/85	195/85	Reverse	182/38	284/15	31/48
H61	16.553	106.958	200/50	200/50	Reverse	352/2	262/29	87/60
H109	15.849	107.698	325/68	20/55	Reverse	350/16	250/32	102/53
H109	15.849	107.698	320/80	35/40	Sinistral reverse	355/19	242/49	99/35
H155	16.469	107.441	230/50	210/45	Reverse	20/4	287/33	116/57
Strike-slip fault with northwest-southeast compressional direction								
H05	17.099	106.553	190/68	125/45	Reverse	324/12	203/67	58/19
H62	16.536	106.961	190/75	105/25	Dextral	150/6	251/61	57/28
H62	16.536	106.961	10/65	90/20	Dextral normal	139/31	329/58	232/5
H62	15.536	106.961	05/75	85/25	Dextral	138/28	304/61	45/6
H109	15.849	107.698	265/75	5/5	Sinistral	132/14	284/74	40/7
H115	15.881	107.804	175/90	75/28	Dextral normal	134/19	265/62	39/16
H111	15.862	107.726	356/63	285/24	Dextral reverse	136/4	40/54	228/35
H183	16.141	108.107	200/90	103/15	Dextral	156/10	290/75	64/11
H183	16.141	108.107	185/65	100/10	Dextral	320/11	208/63	55/24
H183	16.141	108.107	168/70	85/5	Dextral	302/11	182/69	36/17
H200	15.876	107.861	280/88	10/25	Sinistral	322/16	194/65	57/19
H200	15.876	107.861	280/85	10/22	Sinistral	322/12	202/67	56/19
H184	16.139	108.111	290/80	220/45	Normal	149/38	10/44	257/22

https://doi.org/10.1007/s12303-021-0006-6

Table 3. (continued)

Outcrop No.	Coordinates		Attitude of slip surface (azimuth of dip direction/dip angle)	Attitude of striation (azimuth of dip direction/dip angle)	Movement direction	Principal stress vector (azimuth of stress axis/inclination of stress axis) (degree)		
	Latitude (degree)	Longitude (degree)				σ_1	σ_2	σ_3
Reverse - strike-slip fault and reverse fault with northwest-southeast compressional direction								
H43	16.869	106.573	345/40	345/40	Reverse	131/14	33/29	244/56
H99	15.943	107.573	160/75	90/55	Reverse	134/22	240/34	17/48
H104	15.889	107.647	140/70	73/85	Sinistral	136/25	228/5	328/65
H90	15.869	107.480	25/35	300/10	Reverse	151/31	37/34	271/41
H90	15.869	107.480	5/15	300/10	Reverse	118/41	15/15	270/46
H109	15.849	107.698	310/86	40/65	Reverse	332/36	222/25	106/44
H109	15.849	107.698	325/90	325/90	Reverse	325/45	55/0	145/45
Reverse - strike-slip fault and reverse fault with northwest-southeast compressional direction								
H108	15.841	107.688	240/35	175/18	Sinistral	131/45	262/33	11/27
H108	15.841	107.688	5/70	75/38	Normal	138/41	299/48	39/10
Strike-slip fault with sub-latitudinal compressional direction								
H111	15.862	107.726	150/70	85/5	Dextral	284/11	164/69	18/17
H115	15.881	107.804	220/78	295/20	Sinistral	262/5	160/67	354/23
H155	16.469	107.441	235/58	315/15	Sinistral	99/13	208/55	1/32
H194	15.826	107.669	145/88	230/25	Dextral normal	282/19	59/65	187/16
H203	16.494	107.357	60/50	60/50	Reverse	267/2	358/29	173/60
Reverse - strike-slip fault with sub-latitudinal compressional direction								
H108	15.841	107.688	240/35	280/25	Reverse	105/24	210/31	344/49
H110	15.861	107.725	145/55	75/35	Dextral reverse	289/4	196/42	24/48
Normal fault, strike-slip - normal fault with sub-latitudinal compressional direction								
H65	16.395	107.063	335/20	6/5	Dextral	80/43	330/20	222/40
H110	15.861	107.725	215/52	155/35	Normal	97/49	264/40	359/7
H157	16.491	107.465	95/78	155/70	Normal	251/53	09/20	111/30
H157	16.491	107.465	120/76	155/70	Normal	275/55	35/19	136/28
H109	15.849	107.698	340/70	65/25	Dextral normal	111/32	286/58	20/2
H110	15.861	107.725	225/65	150/20	Sinistral	96/31	266/58	3/5
Strike-slip fault with northeast-southwest compressional direction								
H02	17.118	106.586	95/80	5/10	Dextral	51/3	159/79	320/11
H99	15.943	107.572	160/75	80/26	Sinistral	27/29	222/60	120/7
H157	16.491	107.465	95/78	13/30	Dextral	56/11	165/58	320/30
H184	16.139	108.111	280/80	185/15	Dextral	237/3	337/72	146/18
H185	16.134	108.108	260/77	355/15	Dextral	33/20	210/70	303/1
Reverse fault with northeast-southwest compressional direction								
H53	16.593	106.927	220/89	220/89	Reverse	219/44	310/1	41/46
H61	16.553	106.958	200/80	270/60	Reverse	224/29	116/29	349/47
H65	16.395	107.063	240/86	240/86	Reverse	236/41	330/4	64/49
H203	16.494	107.357	50/70	50/70	Reverse	65/22	327/19	201/60
Normal fault with northeast-southwest compressional direction								
H65	16.395	107.063	310/20	245/8	Dextral	208/44	319/20	66/39

The Truong Son fault zone is found at the outcrop H49, in the Rao Quan river bed, Huong Tan commune, Huong Hoa district, Quang Tri province (Fig. 3). The Truong Son shear zone follows the west northwest-east southeast direction, slips dextrally and makes the quartz-sericite schist of A Vuong formation ($\in_2$–O_1av) convex towards northeast on the southwest wall (Fig. 6a). At the outcrop H57, in Dakrong commune, Dakrong district, Quang Tri province (Fig. 3), the Truong Son shear zone has the extremely steep altitude towards the northeast (20–30/80) and destroys the gneiss of A Vuong formation ($\in_2$–O_1av) (Fig. 6b).

The Nam O-Nam Dong fault zone is found at the outcrop H178, in Huong Loc commune, Nam Dong district, Thua Thien

Hue province (Fig. 3). Here the latitudinal gorge coincides with the Nam O-Nam Dong fault zone. The Nam O-Nam Dong fault zone has the extremely steep altitude towards the south (180–185/70–80) and destroys the quartz-sericite of Long Dai formation (O_3–S_1ld) (Fig. 6c).

Among the surveyed fractures, there are hundreds of fractures with the manifestation of slip. They cause the edge dislocation of the pebbles which they cut through, or leave striations on the slip surfaces. Typically, the northeast-southwest fracture zone with the altitude 145/78–85 cuts through the polymictic, poorly-rounded, poorly-sorted, weakly-consolidated pebble beds with the pebble size ranging from 1 cm to 10–15 cm, and causes the left-lateral dislocation of the edge of pebbles with the northwest-southeast extending direction, in the Pliocene–Early Pleistocene conglomerate (?) with the amplitude up to 1.5 cm (Fig. 6d). This conglomerate bed forms a second-order terrace, with a relative height of about 20–25 m, on the left bank of Cam Lo River, in Tan Hiep village, Cam Tuyen commune, Cam Lo district, Quang Tri province (the outcrop DM-TK21) (Fig. 3). The undisturbed tektite is also found on the surface of this terrace. These slip movements reflect the strike-slip stress state of Pliocene–Quaternary period with the sub-longitudinal compressional direction.

Based on the data on displacement and the processing of data on slip observed at the outcrops, the different deformation phases have been identified in terms of characteristics of tectonic stress state; accordingly, the kinematics of the faults is also determined (Table 3). Additionally, based on the data on displacement, we have determined the strike-slip tectonic stress state of Pliocene–Quaternary period with the sub-longitudinal compressional direction. It is a new finding about the modern tectonic stress state of North Central Vietnam and it is consistent with the trend of tectonic stress state of the surrounding region (Yem, 1991; Xu, 2001; Heidbach et al., 2018). In this tectonic stress state, the slip mechanisms of fault zones are identified. The northwest-southeast faults follow the dextral strike-slip mechanism; the northeast-southwest faults follow the sinistral strike-slip mechanism; the latitudinal and sub-latitudinal faults develop with the reverse slip mechanism; and the longitudinal and sub-longitudinal faults develop with the normal slip mechanism.

7. CONCLUSIONS

In this study, based on the comprehensive analysis of geomorphic indices, namely drainage basin asymmetry AF, valley floor width-to-height ratio V_f and mountain front sinuosity S_{mf} as well as the results of structural geological and geomorphological surveys, we have made some remarks on the activity of tectonic faults in the North Central Vietnam as follows:

(1) The modern activity of faults in the study area is assessed as moderate–weak. Only a few segments on the Truong Son and Dakrong-Hue faults are assessed as strongly active.

(2) The simultaneous analysis of S_{mf} and V_f also shows that the vertical tectonic activity of this area is averagely weak, with an average uplifting rate of about 0.2 mm/year.

(3) All the faults in the study area have the vertical or extremely steep slip surfaces with a dip angle of 70–90°. Their movements during the neotectonic period occur in strike-slip tectonic stress fields with the horizontal or nearly horizontal compressional force in the latitudinal and sub-latitudinal directions in Eocene–Miocene and in the longitudinal and sub-longitudinal directions from Pliocene to present. It is a new finding of the modern tectonic stress state of North Central Vietnam. The movement mechanism of faults in the North Central Vietnam follows the rule: dextral strike-slip on the northwest-southeast segments, sinistral strike-slip on the northeast-southwest segments, inverse on the latitudinal and sub-latitudinal segments, and normal on the longitudinal and sub-longitudinal segments.

ACKNOWLEDGMENTS

We would like to thank three anonymous reviewers and Dr. Raehee Han for their helpful comments. This work has been supported by the National-level Independent Project DTDL.CN.51/16.

REFERENCES

Azor, A., Keller, E.A., and Yeats, R.S., 2002, Geomorphic indicators of active fold growth: South Mountain-Oak Ridge anticline, Ventura basin, southern California. Geological Society of America Bulletin, 114, 745–753.

Bagha, N., Arian, M., Ghorashi, M., Pourkermani, M., El Hamdouni, R., and Solgi, A., 2014, Evaluation of relative tectonic activity in the Tehran basin, central Alborz, northern Iran. Geomorphology, 213, 66–87.

Bishop, P., 2007, Long-term landscape evolution: linking tectonics and surface processes. Earth Surface Processes and Landforms, 32, 329–365.

Bull, W.B. and McFadden, L.D., 1977, Tectonic geomorphology north and south of the Garlock fault, California. In: Doehering, D.O. (ed.), Geomorphology in Arid Regions. Routledge, London, p. 115–137.

Cox, R.T., 1994, Analysis of drainage-basin symmetry as a rapid technique to identify areas of possible Quaternary tilt-block tectonics: an example from the Mississippi Embayment. Geological Society of America Bulletin, 106, 571–581.

Dehbozorgi, M., Pourkermani, M., Arian, M., Matkan, A.A., Motamedi, H., and Hosseiniasl, A., 2010, Quantitative analysis of relative tectonic activity in the Sarvestan area, central Zagros, Iran. Geomorphology, 121, 329–341.

Duong, N.A., Nguyen, P.D., Tuan, V.M., Duan, B.V and Linh, N.T., 2017,

https://doi.org/10.1007/s12303-021-0006-6

Seismic hazard assessment and local site effect evaluation in Hanoi, Vietnam. Journal of Marine Science and Technology, 17, 82–95. https://doi.org/10.15625/1859-3097/17/4B/12996

Duong, N.A., Sagiya, T., Kimata, F., To, T.D., Hai, V.Q., Cong, D.C., Binh, N.X., and Xuyen, N.D., 2013, Contemporary horizontal crustal movement estimation for northwestern Vietnam inferred from repeated GPS measurements. Earth Planets Space, 65, 1399–1410.

El Hamdouni, R., Irigaray, C., Fernández, T., Chacón, J., and Keller, E.A., 2008, Assessment of relative active tectonics, southwest border of the Sierra Nevada (southern Spain). Geomorphology, 96, 150–173.

Giaconia, F., Booth-Rea, G., Martinez-Martinez, J.M., Azanon, J.M., Perez-Pena, J.V., Perez-Romero, J., and Villegas, I., 2012, Geomorphic evidence of active tectonics in the Sierra Alhamilla (eastern Betics, SE Spain). Geomorphology, 145–146, 90–106.

Hare, P.W. and Gardner, T.W., 1985, Geomorphic indicators of vertical neotectonism along converning plate margins, Nicoya Peninsula, Costa Rica. In: Morisawa, M. and Hack, J.T. (eds.), Tectonic Geomorphology. Proceedings of the 15th Annual Geomorphology Symposium, Binghamton, Sep. 1984, p. 75–104. https://doi.org/10.1002/gj.3350210222

Heidbach, O., Rajabi, M., Cui, X., Fuchs, K., Müller, B., Reinecker, J., Reiter, K., Tingay, M., Wenzel, F., Xie, F., Ziegler, M.O., Zoback, M.-L., and Zoback, M., 2018, The World Stress Map database release 2016: crustal stress pattern across scales. Tectonophysics, 744, 484–498. https://doi.org/10.1016/j.tecto.2018.07.007

Hung, P.N., Trong, C.D., Dung, L.V., Tuan, T.A., Bach, M.X., and Duong, N.A., 2019, Study on structure of the Earth's crust in Thua Thien–Hue province and adjacent areas by using gravity and magnetic data in combination. Vietnam Journal of Marine Science and Technology, 19, 517–526. https://doi.org/10.15625/1859-3097/19/4/14903

Husson, L., Bodin, T., Spada, G., Choblet, G., and Comé, K., 2018, Bayesian surface reconstruction of geodetic uplift rates: mapping the global fingerprint of glacial isostatic adjustment. Journal of Geodynamics, 122, 25–40.

Keller, E.A. and Pinter, N., 2002, Active Tectonics: Earthquakes, Uplift, and Landscape (2nd edition). Prentice Hall, Upper Saddle River, 362 p.

Lacassin, R., Maluski, H., Leloup, P.H., Tapponnier, P., Hinthong, C., Siribhakdi, K., Chuaviroj, S., and Charoenravat, A., 1997, Tertiary diachronic extrusion and deformation of western Indochina: structural and $^{40}Ar/^{39}Ar$ evidence from NW Thailand. Journal of Geophysical Research, 102, 10013–10037.

Mahmood, S.A. and Gloaguen R., 2012, Appraisal of active tectonics in Hindu Kush: insights from DEM derived geomorphic indices and drainage analysis. Geoscience Frontiers, 3, 407–428.

Malik, J.N. and Mohanty, C., 2007, Active tectonic influence on the evolution of drainage and landscape: geographic signatures from frontal and hinterland areas along the north-western Himalaya, India. Journal of Asian Earth Sciences, 29, 604–618.

Minh, L.H., 2015, Studying seismic impacts on the stability of Song Tranh 2 dam in Bac Tra My area, Quang Nam province. Final report of the National project DTDL.2013-G (2013–2016), Institute of Geophysics, Vietnam Academy of Science and Technology, Hanoi, 412 p. (in Vietnamese)

Morley C.K., 2004, Nested strike-slip duplexes, and other evidence for Late Cretaceous–Palaeogene transpressional tectonics before and during India-Eurasia collision, in Thailand, Myanmar and Malaysia. Journal of the Geological Society, 161, 799–812.

Ozkaymak, C. and Sozbilir, H., 2012, Tectonic geomorphology of the Spildagi high ranges, western Anatolia. Geomorphology, 173–174, 128–140.

Pavano, F., Pazzaglia, F.J., and Catalano, S., 2016, Knickpoints as geomorphic markers of active tectonics: a case study from northeastern Sicily (southern Italy). Lithosphere, 8, 633–648.

Perez-Pena, J.V., Azor, A., Azanon, J.M., and Keller, E.A., 2010, Active tectonics in the Sierra Nevada (Betic Cordillera, SE Spain): insights from geomorphic indexes and drainage pattern analysis. Geomorphology, 119, 74–87.

Phuong, N.H. and Truyen, P.T., 2014, Probabilistic seismic hazard assessment for the South Central Vietnam. Vietnam Journal of Earth Sciences, 36, 451–461. https://doi.org/10.15625/0866-7187/36/4/6433

Ramirez-Herrera, M.T., 1998, Geomorphic assessment of active tectonics in the Acambay graben, Mexican Volcanic Belt. Earth Surface Processes and Landforms, 23, 317–332.

Rockwell, T.K., Keller, E.A., Clark, M.N., and Johnson, D.L., 1984, Chronology and rates of faulting of Ventura River terraces, California. Geological Society of America Bulletin, 95, 1466–1474.

Scotti, V.N., Molin, P., Faccenna, C., Soligo, M., and Casas-Sainz, A., 2014, The influence of surface and tectonic processes on landscape evolution of the Iberian Chain (Spain): quantitative geomorphological analysis and geochronology. Geomorphology, 206, 37–57.

Sharma, G., Champatiray, P.K., and Mohanty, S., 2018, Morphotectonic analysis and GNSS observations for assessment of relative tectonic activity in Alaknanda basin of Garhwal Himalaya, India. Geomorphology, 301, 108–120.

Silva, P.G., Goy, J.L., Zazo, C., and Bardaji, T., 2003, Fault-generated mountain fronts in southeast Spain: geomorphologic assessment of tectonic and seismic activity. Geomorphology, 50, 203–225.

Summerfield, M.A., 2000, Geomorphology and Global Tectonics. John Wiley & Sons, Chichester, 386 p.

Tapponnier, P., Peltzer, P., Le Dain, A.Y., Armijo, R., and Cobbold, P., 1982, Propagating extrusion tectonics in Asia: new insights from simple experiments with plasticine. Geology, 10, 611–616.

Thom, B.V., 2001, Defining character activity of Huong Hoa-A Luoi fault zone by method of three conjugate fractures analysis. Vietnam Journal of Earth Sciences, 23, 246-253. (in Vietnamese with English abstract). https://doi.org/10.15625/0866-7187/23/3/11338

Thom, B.V., 2002, Some features of neo-tectonic faults in North Central region. Ph.D. Thesis, Institute of Geology, Hanoi 118 p. (in Vietnamese)

Thuy, N.N. (ed.), 2005, Assessment of seismic hazard and earthquake micro-zoning in Huong Dien hydropower plant area (Technical design stage). Final report of project. Institute of Geophysics, Vietnam Academy of Science and Technology, Hanoi, 83 p. (in Vietnamese)

Thuy, N.N. (ed.), 2007, Assessment of earthquake - tectonics of Da Mai - Tan Kim hydropower plant project, Quang Tri province (Investment project stage). Final report of project. Institute of Geophysics, Vietnam Academy of Science and Technology, Hanoi, 69 p. (in Vietnamese)

Tien, P.C. (ed.), 1991, Geological map of Cambodia-Laos-Vietnam (1:1,000,000). Geological Survey of Vietnam, Hanoi. (in Vietnamese)

Trang, N.V., 1996, Geological and mineral resources map of Huong Hoa-Hue-Da Nang sheet (1:200,000). Department of Geology and Minerals of Vietnam, Hanoi, 94 p. (in Vietnamese)

Troiani, F., Galve, J.P., Piacentini, D., Della Seta, M., and Guerrero, J., 2014, Spatial analysis of stream length-gradient (SL) index for detecting hillslope processes: a case of the Gállego River headwaters (central Pyrenees, Spain). Geomorphology, 214, 183–197.

Tsodoulos, I.M., Koukouvelas, I.K., and Pavlides, S., 2008, Tectonic geomorphology of the easternmost extension of the Gulf of Corinth (Beotia, Central Greece). Tectonophysics, 453, 211–232.

Wells, S.G., Bullard, T.F., Menges, C.M., Drake, P.G., Karas, P.A., Kelson, K.I., and Wesling, J.R., 1988, Regional variations in tectonic geomorphology along a segmented convergent plate boundary pacific coast of Costa Rica. Geomorphology, 1, 239–265.

Xu, Z., 2001, A present-day tectonic stress map for eastern Asia region. Acta Seimologica Sinica, 14, 524–533. https://doi.org/10.1007/BF02718059

Xuan, P.T., Duong, N.A., Van Chinh, V., Dang, P. T., Qua, N.X., and Van Pho, N., 2020, Soil gas radon measurement for identifying active faults in Thua Thien Hue (Vietnam). Journal of Geoscience and Environment Protection, 8, 44–64. https://doi.org/10.4236/gep.2020.87003

Xuyen, N.D., 2004, Study on earthquake prediction and ground motion in Vietnam. Final report of the National project 2000–2002, Institute of Geophysics, Vietnam Academy of Science and Technology, Hanoi. (in Vietnamese)

Xuyen, N.D. and Thuy, N.N., 1996, Database for solutions to mitigate consequences of earthquakes in Vietnam. Final report of the National project 1994–1996, Institute of Geophysics, Vietnam Academy of Science and Technology, Hanoi, 117 p. (in Vietnamese)

Yem, N.T., 1991, Neotectonic stress fields of Red River Trough. Geology-Resources, Institute of Geology, Sciences and Technics Publishing House, Hanoi, 165 p. (in Vietnamese with English abstract)

Yem, N.T., 2005, Research on soil cracking in Vietnam and solutions of prevention and mitigation of damage. Summary report on basic, independent, state-level investigation project, code: DL.94, Archives of the National Science and Technology Information Administration, Hanoi, 57 p. (in Vietnamese)

Yin, A., 2010, Cenozoic tectonic evolution of Asia: a preliminary synthesis. Tectonophysics, 488, 293–325.

https://doi.org/10.1007/s12303-021-0006-6